



Published in final edited form as:

*Laryngoscope*. 2024 March ; 134(3): 1363–1371. doi:10.1002/lary.30936.

## Cochlear Nucleus Transcriptome of a Fragile X Mouse Model Reveals Candidate Genes for Hyperacusis

**Hitomi Sakano, MD, PhD,**

Department of Otolaryngology, University of Rochester Medical Center, Rochester, New York, USA, Department of Neuroscience, University of Rochester Medical Center, Rochester, New York, USA, Center for RNA Biology, University of Rochester, Rochester, New York, USA

**Michael S. Castle, MD,**

Department of Otolaryngology, University of Rochester Medical Center, Rochester, New York, USA

**Paromita Kundu, PhD**

Department of Otolaryngology, University of Rochester Medical Center, Rochester, New York, USA

### Abstract

**Objective:** Fragile X Syndrome (FXS) is a hereditary form of autism spectrum disorder. It is caused by a trinucleotide repeat expansion in the *Fmr1* gene, leading to a loss of Fragile X Protein (FMRP) expression. The loss of FMRP causes auditory hypersensitivity: FXS patients display hyperacusis and the *Fmr1*-knock-out (KO) mouse model for FXS exhibits auditory seizures. FMRP is strongly expressed in the cochlear nucleus and other auditory brainstem nuclei. We hypothesize that the *Fmr1*-KO mouse has altered gene expression in the cochlear nucleus that may contribute to auditory hypersensitivity.

**Methods:** RNA was isolated from cochlear nuclei of *Fmr1*-KO and WT mice. Using next-generation sequencing (RNA-seq), the transcriptomes of *Fmr1*-KO mice and WT mice ( $n = 3$  each) were compared and analyzed using gene ontology programs.

**Results:** We identified 270 unique, differentially expressed genes between *Fmr1*-KO and WT cochlear nuclei. Upregulated genes (67%) are enriched in those encoding secreted molecules. Downregulated genes (33%) are enriched in neuronal function, including synaptic pathways, some of which are ideal candidate genes that may contribute to hyperacusis.

**Conclusion:** The loss of FMRP can affect the expression of genes in the cochlear nucleus that are important for neuronal signaling. One of these, *Kcnab2*, which encodes a subunit of the Shaker voltage-gated potassium channel, is expressed at an abnormally low level in the *Fmr1*-KO

---

Send correspondence to Hitomi Sakano, Department of Otolaryngology, University of Rochester Medical Center, 601 Elmwood Ave, Box 629, Rochester, NY 14642, USA. hitomisa@uw.edu.

The authors have no other funding, financial relationships, or conflicts of interest to disclose.

Additional supporting information may be found in the online version of this article.

Level of Evidence:

Level N/A

cochlear nucleus. *Kcnab2* and other differentially expressed genes may represent pathways for the development of hyperacusis. Future studies will be aimed at investigating the effects of these altered genes on hyperacusis.

### Keywords

cochlear nucleus; hyperacusis; FMRP; Fragile X; KCNAB2

## INTRODUCTION

The *Fmr1* gene encodes Fragile X Protein (FMRP), which is an RNA-binding protein that is best characterized as a translational repressor<sup>1</sup> and is important for proper synaptic development.<sup>2</sup> However, a trinucleotide repeat expansion in the 5'-untranslated region of the *Fmr1* gene results in the failure to produce FMRP<sup>3</sup> and is the most common single-gene cause of autism spectrum disorder called Fragile X Syndrome (FXS) with a prevalence of at least 1 in 4000.<sup>4</sup> FXS patients as well as rodent models for FXS can exhibit hypersensitivity to sensory stimulation, including hyperacusis.<sup>5</sup> The well-studied *Fmr1* knock-out (*Fmr1*-KO) mouse<sup>6</sup> exhibits audiogenic seizures in response to loud sounds of 120dB<sup>7,8</sup> and abnormal auditory startle reflexes.<sup>9</sup> Thus, this mouse may serve as a useful model for studying auditory hypersensitivity, a condition whose mechanism of pathogenesis is not well understood.

A recent study suggests that subcortical excitatory neurons of the auditory pathway are necessary for the audiogenic seizure phenotype of *Fmr1*-KO mice.<sup>10</sup> Although FMRP is widely expressed throughout the brain, it has previously been shown that FMRP is highly concentrated in auditory brainstem nuclei of mice, including the cochlear nucleus.<sup>11</sup> We hypothesized that the loss of FMRP may result in gene expression changes in the auditory brainstem that may contribute to auditory hypersensitivity.

Here, we present a transcriptomic comparison of the *Fmr1*-KO and wild-type (WT) cochlear nucleus to provide an initial survey of potential genes whose dysregulation upon *Fmr1*-KO may contribute to hyperacusis. Candidate genes of interest encode proteins that are important for neuronal activity or synaptic modulation. Among these, we further characterize *Kcnab2* which encodes a  $\beta$ -subunit that modulates the activity of the  $\alpha$  subunits of the Shaker potassium channel family that are important for the faithful transmission of auditory signals along the auditory pathway.<sup>12-14</sup> Thus, the reduction of *Kcnab2* may contribute to auditory hypersensitivity seen in the *Fmr1*-KO mouse.

## MATERIALS AND METHODS

### Animals

Animals were used in compliance with a protocol approved by the University Committee on Animal Resources. Two-month-old male mice were used for all experiments unless otherwise specified. *Fmr1*-KO mice from Jackson Laboratory (B6.129P2-*Fmr1*<sup>tm1Cgr</sup>/J, #003025) in the C57Bl/6J strain (#000664) were maintained with intermittent backcrossing to C57Bl/6J.

## RNA Sequencing/Analysis

Cochlear nuclei (dorsal and ventral) were dissected from fresh brainstem sections. For each *Fmr1*-KO and WT, three biological replicates were prepared (two male mice pooled for each replicate). Tissues were homogenized in lysis buffer (10 mM TrisHCl, 150 mM NaCl, 10 mM EDTA, 0.5% Triton™ X-100) and RNA purified with RNeasy Mini kits with DNase I digestion (QIAGEN). RNA-seq libraries were constructed using TruSeq Stranded mRNA Library Prep Kit (Illumina) with 200 ng of RNA. The quantity and quality of libraries were measured using a Qubit 4 Fluorometer (Thermo Fisher Scientific) and a 5300 Fragment Analyzer System (Agilent), respectively. Sequencing performed on Illumina NextSeq550. Raw reads generated from the Illumina base calls were demultiplexed using bcl2fastq version 2.19.1. Quality filtering and adapter removal were performed using FastP version 0.20.0 with parameters “--length\_required 35 --cut\_front\_window\_size 1 --cut\_front\_mean\_quality 13 --cut\_front --cut\_tail\_window\_size 1 --cut\_tail\_mean\_quality 13 --cut\_tail -w 8 -y -r -j”. Cleaned reads were aligned to the *Mus musculus* reference genome (GRCm38.p6 + Gencode-M22 Annotation) using STAR\_2.7.0f and parameters “--twopassMode Basic --runMode alignReads --genomeDir \${GENOME} --readFilesIn \${SAMPLE} --outSAMtype BAM Unsorted --outSAMstrandField intronMotif voutFilterIntronMotifs RemoveNoncanonical”. For RNA-seq analyses, gene-level read quantification was derived using the subread-1.6.4 package (featureCounts) with a GTF annotation file (Gencode M22) and parameters “-s 2 -t exon -g gene\_name”. For comparative transcript expression analyses, transcript-level reads were quantified with Salmon-0.13.1. Data normalization and differential expression analysis between wildtype and *Fmr1*-KO groups were performed using DESeq2-1.22.1 using median of ratios normalization, an adjusted P-value threshold of 0.05 within R version 3.5.1 (<https://www.R-project.org/>). Pheatmap version 1.0.12 (<https://CRAN.R-project.org/package=pheatmap>) was used to produce the heatmap of differentially expressed genes. The RNA-seq raw data is available through GEO, accession number GSE236056 (<https://www.ncbi.nlm.nih.gov/geo/query/acc.cgi?acc=GSE236056>). Gene ontology analysis utilized DAVID program (<https://david.ncifcrf.gov/>),<sup>15</sup> The Human Protein Atlas (<https://www.proteinatlas.org/>) and EMBL-EBI expression atlas (<https://www.ebi.ac.uk/gxa/home>).

## Reverse Transcription Quantitative Polymerase Chain Reaction (RT-qPCR)

RNA (250 ng), isolated as described above, was reverse transcribed using qScript cDNA SuperMix (Quantabio), and 1/100th of it was used in 10 µl quantitative (q)PCR reactions that employed SYBR™ Select Master Mix (Thermo Fisher Scientific). PCR was undertaken using a QuantStudio™ Real-Time PCR System (Thermo Fischer Scientific) using serial dilution control using WT samples. Quantitation was performed using the standard curve method and Pfaffl calculation using Microsoft Excel. The following primers were utilized: *Kcnab2* forward (CTGCAGCTGGAGTACGTGG), *Kcnab2* reverse (CATCCCCTGGTTGATGACA), *Actb* forward (CGCCACCAGTTCGCCATGGA), and *Actb* reverse (TACAGCCCGGGGAGCATCGT). Cycling conditions: 94°C for 2 min, followed by 40 cycles at 94°C for 15 s and 60°C for 1 min.

## Western Blotting

Dissected cochlear nuclei were homogenized with a pestle in 6 M urea, sonicated for 10 s, and centrifuged at  $14,000 \times g$  for 10 min to remove cellular debris. Protein was quantitated using Bradford Assay (Bio-Rad). Western blotting was performed as described<sup>16</sup> using 10  $\mu$ g of protein per lane. See Table I for primary antibody concentrations. Horseradish peroxidase-conjugated goat secondary antibody was used at 1:30,000 dilution (Abcam ab6721). Blots were developed using Pierce<sup>TM</sup> SuperSignal<sup>TM</sup> West Pico Western Blot Kit (Thermo Scientific) and imaged with ChemiDoc<sup>TM</sup> Touch Imaging System (Bio-Rad).

## Immunostaining

CO<sub>2</sub> euthanized mice were perfused with phosphate-buffered saline (PBS) (137 mM NaCl, 2.7 mM KCl, 10 mM Na<sub>2</sub>HPO<sub>4</sub>, and 1.8 mM KH<sub>2</sub>PO<sub>4</sub>) followed by fixative (4% paraformaldehyde in PBS). Brains were postfixed for 2 h, dehydrated in 30% sucrose/PBS for 72 h, and frozen in O.C.T. Medium (Sakura). Cryosections (14  $\mu$ m) of cochlear nucleus were collected (Leica CM1860 UV) and mounted on SuperFrost glass slides (Fisher Scientific). Slides were incubated sequentially in Tris-buffered saline (TBS) (50 mM Tris HCl, 150 mM NaCl, pH 7.5), TBS with 0.1% Triton<sup>TM</sup> X-100 and TNB Blocking Buffer (Perkin Elmer) with 0.1% Triton<sup>TM</sup> X-100. See Table I for the primary antibodies used. Antibody incubations were performed in TNB Blocking Buffer. Rabbit antibodies were detected with Alexa-488-conjugated goat antibody (1:500, Invitrogen A11034). Mouse antibodies were detected with an M.O.M. kit (Vector) and streptavidin-Cy3 (1:1000). Following washing in TBS, slides were mounted using Fluoromount-G<sup>TM</sup> (Invitrogen) and imaged using a Zeiss Palm MicroBeam microscope. Images were analyzed with Image J software. For each WT and *Fmr1*-KO, 20 $\times$  images of four ventral cochlear nuclei from equivalent cross-sections were analyzed. Within each nucleus, a 600  $\times$  600 pixel square region was selected. For cell intensity measurement, the same fixed circle shape was used to measure average pixel intensity within the cell body of a stained neuron. Statistics were performed using Microsoft Excel.

## RESULTS

Consistent with previous literature,<sup>8</sup> *Fmr1*-KO mice exhibit seizures to >120 dB sound. Wild running and/or grand mal seizures were observed in 10/14 (71%) *Fmr1*-KO mice and in 0/11 (0%) WT mice (Supplemental Table 1). FMRP is readily detected by immunostaining in the cochlear nucleus of adult WT mice (Fig. 1A) but not of *Fmr1*-KO (Fig. 1B). We dissected cochlear nuclei (both ventral and dorsal) from two-month-old WT and *Fmr1*-KO male mice (Fig. 1C, dotted outline, identified in comparison to an intact nucleus Fig. 1D).

Transcriptome analysis of cochlear nuclei between WT and *Fmr1*-KO ( $n = 3$  each) reveal 286 transcripts that were differentially expressed between the two genotypes (Fig. 2A), of which, 270 were unique (Supplemental Table 2). FMRP is known to bind mRNA transcripts which have been previously defined by cross-linking immunoprecipitation using FMRP specific antibody and mouse brain.<sup>17,18</sup> We found that only 21 of 270 transcripts are known FMRP bound targets, therefore, a majority of altered gene expression is likely indirectly of FMRP binding. Interestingly, FMRP target genes tended to be downregulated more than

non-FMRP target genes (leftward shift in the distribution of genes with given log<sub>2</sub> fold difference in Fig. 2B), suggesting that loss of FMRP binding may reduce the stability of FMRP target mRNAs.

To select the most differentially expressed genes, cut-off differentials were set to  $|\log_2$  fold change|  $\geq 0.5$  and p-value of  $<0.001$  (Fig. 2C, red and blue box on the volcano plot). This yielded 142 genes, 67% of which were upregulated, and 33% of which were downregulated in *Fmr1*-KO relative to WT mice (Fig. 2D). Gene ontology analysis reveals that upregulated genes were enriched in those encoding secreted proteins. Interestingly, among the 38 genes that fell into the category of secreted and extracellular pathways, 30 are expressed in immune or glial cells (Supplemental Table 3), which are involved in the supportive and maintenance function of the nervous system. Several other upregulated genes encode proteins that function in transcriptional regulation.

Downregulated genes in *Fmr1*-KO cochlear nucleus were enriched in those involved in synaptic pathways. Genes encoding proteins in the synapse were of particular interest because of their ability to affect neuronal activity. Among them include: *Piezo1*, *Kcnp4*, *Gria3*, *Kcnab2*, *Clcn7* and *Pacsin1* (Table II). Gene search through the Allen Brain Atlas<sup>21</sup> (online in-situ hybridization database) reveals that all genes are expressed in mouse cochlear nucleus (data not shown).

We chose to further characterize *Kcnab2* which had the highest expression level among the candidate genes. RT-qPCR confirmed the decreased gene expression from 1.06 (95% CI [0.88,1.23],  $n = 6$ ) in WT to 0.75 (95% CI [0.66,0.84],  $n = 7$ ) in *Fmr1*-KO cochlear nuclei, ( $p < 0.01$ , Student's t-test) (Fig. 3). Transcript abundance was normalized to the abundance of a control gene *Actb* (a.k.a.,  $\beta$ -actin) transcript that was stable between samples.

We examined the tissue expression of KCNAB2 protein using immunostaining. The specificity of the KCNAB2 antibody used was confirmed by western blotting, which recognized the expected 44-kDa band that was decreased in the *Fmr1*-KO cochlear nucleus lysate (Fig. 4A). Immunostaining showed that only a subset of neurons in the cochlear nucleus express KCNAB2 (Fig. 4B, arrows) in both ventral and dorsal cochlear nuclei. There is also punctate staining along neurites (Fig. 4B, arrowhead). Furthermore, a comparison of *Fmr1*-KO to WT animals showed a similar pattern of expression but a general reduction in the intensity of KCNAB2 immunoreactivity within cells (Fig. 4C). Average pixel intensities were measured from the cell bodies of WT (152.95, 95% CI [146.24,159.66],  $n = 41$ ) and *Fmr1*-KO cells (131.51, 95% CI [127.33,135.69],  $n = 35$ ), revealing a 21 point reduction in the pixel intensity within immunopositive cells that is statistically significant ( $p < 0.01$ , Student's t-test) (Fig. 4D).

Previous studies have shown that KCNAB2 associates *in vitro* with multiple Shaker channel  $\alpha$  subunits, (KCNAB1–3, 5 and 6).<sup>24</sup> We sought to determine which  $\alpha$  subunits may be co-expressed to partner with KCNAB2. We mined the RNA-seq data and found that *Kcna1* and *Kcna2* were highly expressed while *Kcna6* is expressed at much lower levels (Fig. 5A). There was no statistically significant difference between *Fmr1*-KO and WT mice by Student's t-test ( $n = 3$  each). Co-immunohistochemistry in WT ventral cochlear nuclei

was performed to detect KCNAB2 and KCNA1, 2 or 6 (Fig. 5B–J). KCNAB2+ cells (Fig. 5B,D) frequently co-expressed KCNA1 (Fig. 5B,C). KCNAB2+ cells (Fig. 5E,G) also frequently co-expressed KCNA2 (Fig. 5E,F). The distribution of KCNA2 was more localized to the plasma membrane and less so in the cytoplasm when compared with KCNA1 staining pattern. KCNA6 was not detected to be co-expressed with KCNAB2 (Fig. 5H–J). KCNAB2+ cell counting reveals that approximately one-third of co-stains for KCNA1 and one-third for KCNA2 (Fig. 5K).

## DISCUSSION

The *Fmr1*-KO mouse is a well-studied and widely used animal model for FXS. There are numerous reported abnormalities in the *Fmr1*-KO mouse that suggest an auditory processing defect. For example, the *Fmr1*-KO mouse exhibits elevated auditory brainstem response thresholds,<sup>26</sup> abnormalities in acoustic startle reflex,<sup>9</sup> enhanced pre-pulse inhibition,<sup>27</sup> and seizures in response to loud sounds.<sup>7</sup> Loss of FMRP specifically in glutamatergic neurons of the inferior colliculus and brainstem has been reported to be necessary for the audiogenic seizure phenotype.<sup>10</sup> Although the mechanism leading to tinnitus and hyperacusis are not well understood, there is growing evidence to support the central gain enhancement model, where hearing loss or ototoxicity lead to abnormally increased responses in the auditory and central pathways.<sup>20</sup> Consistent with this, the *Fmr1*-KO mouse cortical electrophysiological recordings show hyper-responsiveness to sounds.<sup>26</sup>

To begin to identify candidate genes that contribute to auditory hypersensitivity in the *Fmr1*-KO mouse, we performed transcriptome analyses to define genes that are differentially expressed in the cochlear nucleus of this mouse relative to its WT counterpart. Differentially expressed genes that are upregulated in the *Fmr1*-KO are enriched in those encoding secreted proteins. Interestingly, gene ontology reveals that most of these secreted molecules are expressed in glial cells. There is increasing evidence that glia plays an important role in modulating neuronal activity by pruning and modifying synapses.<sup>28</sup> One-third of genes are found to be downregulated in the *Fmr1*-KO mouse and were enriched in genes encoding proteins that function in synaptic pathways.

Interestingly, transcripts known to be bound by FMRP tended to be more downregulated (50%) compared to those not bound by FMRP (33%), which suggests that the loss of FMRP binding may destabilize or reduce the abundance of FMRP-bound transcripts. Although the sample size is small, this observation is consistent with other transcriptome studies in brain.<sup>19</sup> Downregulated genes also were enriched in those involved in synaptic pathways. Among these, we chose *Kcnab2* as a promising candidate because of its relatively abundant expression and its potential to affect neuronal activity in the cochlear nucleus as a voltage-gated potassium channel subunit. In this study, *Kcnab2* mRNA and KCNAB2 protein were indeed moderately decreased in the *Fmr1*-KO mouse with statistical significance. *Kcnab2* mRNA has not been shown to be bound by FMRP in the brain, thus its reduction in abundance could be due to the indirect effects of FMRP on gene expression. More studies will be needed to determine the exact mechanism.

## What is KCNAB2?

KCNAB2 is an auxiliary  $\beta$  subunit that interacts with multiple members of the pore-forming  $\alpha$  subunits of the Shaker family voltage-gated potassium channels.<sup>24</sup> Shaker channels are important for maintaining the fidelity of high spiking signals along the auditory pathway that can affect auditory behavior.<sup>12–14</sup> Dendrotoxin inhibition of Shaker channel currents results in hyperexcitability of auditory neurons.<sup>12</sup> The  $\alpha$  subunits have six transmembrane domains: the first four are the voltage sensing, and the last two form the pore. These subunits form a heterotetramer.<sup>29</sup> There are multiple members of Shaker family potassium channels (KCNA1, 2, 3, and 6) expressed in rat cochlear nucleus.<sup>25</sup> In rats, KCNA1 (Kv1.1) and KCNA2 (Kv1.2) channels are expressed in bushy and octopus cells in the ventral cochlear nucleus, and in giant and pyramidal cells in the dorsal cochlear nucleus.<sup>30</sup> Our RNA-seq data confirms that *Kcna1*, *2* and *6* are expressed in mouse cochlear nucleus. This study reveals that KCNAB2 is co-expressed in cochlear nucleus neurons with KCNA1 and KCNA2 which are known to interact with KCNAB2.<sup>24</sup> However, co-expression with KCNA6 was not detectable. Approximately one-third of KCNAB2+ cells are not accounted to be co-expressed with an  $\alpha$  subunit. One possibility is that we under-estimated what we considered co-expression based on staining intensity. The other possibility is that KCNA1 and 2 expressions may be more restricted than KCNAB2 expressions.

## What is the Significance of Decreased *Kcnab2* Expression in the *Fmr1*-KO Mouse?

The *Kcnab2* gene is mapped to the 1p36 deletion syndrome which is associated with intellectual delay and epilepsy.<sup>22,23</sup> *Kcnab2*-KO mice have been shown to exhibit susceptibility to seizures.<sup>23</sup> Although auditory brainstem responses have been reported to be statistically no different from WT controls,<sup>23</sup> there is no further study on auditory effects (such as auditory brainstem response amplitudes or latencies and susceptibility to audiogenic seizures). It would be interesting to characterize these mice further.

One study found that KCNAB2 is able to shift the threshold of potassium channel activation by  $-10$  mV without altering inactivation.<sup>31</sup> What would reduction of KCNAB2 abundance be expected to cause? We would expect a loss of KCNAB2 to result in other  $\beta$  subunits such as KCNAB1 to interact with the Shaker potassium channels. KCNAB1, unlike KCNAB2, increases the threshold of channel activation to above the action potential and causes increased inactivation (due to its ball and chain domain)<sup>31</sup> (Fig. 6). The result is prolonged action potential and hyper-excitability due to reduced potassium efflux. Consistent with this, there are reports that deletion of the KCNAB2 subunit causes seizure susceptibility, memory problems, and amygdala hyperexcitability.<sup>23</sup>

## How Does a Decrease in KCNAB2 Abundance in the *Fmr1*-KO Cochlear Nucleus Fit with the Central Gain Enhancement Model?

Although the pathophysiology of hyperacusis and tinnitus are still not well understood, there are findings that support the hypothesis that cochlear damage can lead to maladaptive central responses known as central gain.<sup>20</sup> It is known that there are enhanced responses at the level of the inferior colliculus<sup>34</sup> in response to salicylate treatment used to induce tinnitus. Higher up in the auditory cortex, cochlear damage has been shown to increase the amplitude of cortical response to suprathreshold sounds despite reduced neural input due

to cochlear damage.<sup>35</sup> Single unit recordings do indicate altered spontaneous activity in the cochlear nucleus after an intense tone stimulation.<sup>36,37</sup> Thus, the gain seen at the level of the inferior colliculus may be contributed also by changes in the cochlear nucleus. KCNAB2 expression is also found in other areas of the auditory pathway, including Type I (and to a lesser extent Type II) spiral ganglion neurons,<sup>38,39</sup> cochlear hair cells,<sup>32</sup> and superior olivary complex.<sup>33</sup> Thus, we cannot rule out the possibility that KCNAB2 reduction elsewhere along the auditory pathway could contribute to the auditory seizures.

### Limitations and Potential Future Studies

Considering that the loss of FMRP results in many direct as well as indirect effects, auditory hypersensitivity and auditory seizures in the *Fmr1*-KO mouse are not likely due to the dysregulation of a single gene. While it remains uncertainly, it is likely that KCNAB2 downregulation within the cochlear nucleus of *Fmr1*-KO mice contributes to their auditory hypersensitivity and auditory seizures. Although KCNAB2 is expressed in other cells along the auditory pathway, KCNAB2 in the cochlear nucleus is likely to contribute as well. Future experiments could include tissue-specific knock-down of *Kcnab2* mRNA in WT mice or restoration to normal levels of KCNAB2 in *Fmr1*-KO mice to test for a partial rescue of phenotype. Other experiments may include the characterization of neuronal activity by electrophysiology of KCNAB2-expressing neurons to determine whether there are measurable effects on cochlear nucleus activity in *Fmr1*-KO versus WT animals.

## CONCLUSION

In summary, we have performed an initial comparison of the cochlear nucleus transcriptome in WT and *Fmr1*-KO mice, the latter of which manifest auditory hypersensitivity. Although FMRP is a known mRNA-binding protein, many of the altered genes produce mRNAs that are known not to bind FMRP, which can be explained by indirect effects (i.e., increased translation of FMRP targets causing downstream transcriptional changes). Furthermore, what are normally FMRP-bound mRNAs tended to be downregulated compared to non-FMRP-bound mRNAs in the *Fmr1*-KO mouse, suggesting that FMRP binding to an mRNA may help stabilize bound mRNA. Many of the upregulated genes are expressed in glial cells while many of the downregulated genes are involved in neuronal synaptic pathways. Furthermore, of the several genes whose expression is reduced in *Fmr1*-KO mice and that are involved in synaptic pathways, *Kcnab2* is a promising candidate for further studies in the mechanism of hyperacusis.

## Supplementary Material

Refer to Web version on PubMed Central for supplementary material.

## ACKNOWLEDGMENTS

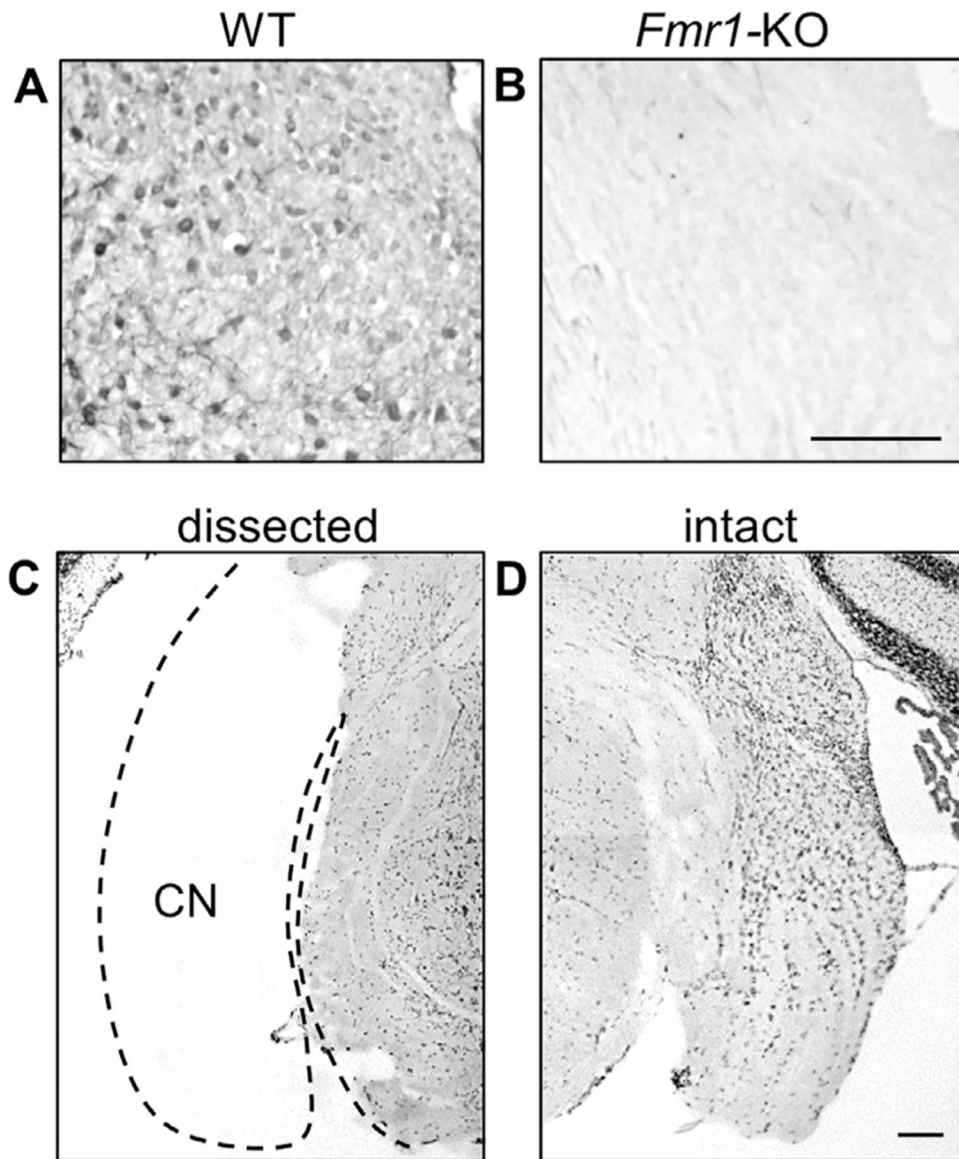
This work was supported by NIH 1K08 DC019416, Schmitt Foundation's Program in Integrative Neuroscience (a part of the Del Monte Institute for Neuroscience Pilot Program), and the Triological Society Career Development Award, all to H.S. Support also derived from University of Rochester core facilities: the University of Rochester Genomics Research Center, the Center for Musculoskeletal Research (NIH P30 AR069655), and Center for Advanced Light Microscopy and Nanoscopy. We thank members of the Maquat lab for helpful discussions.



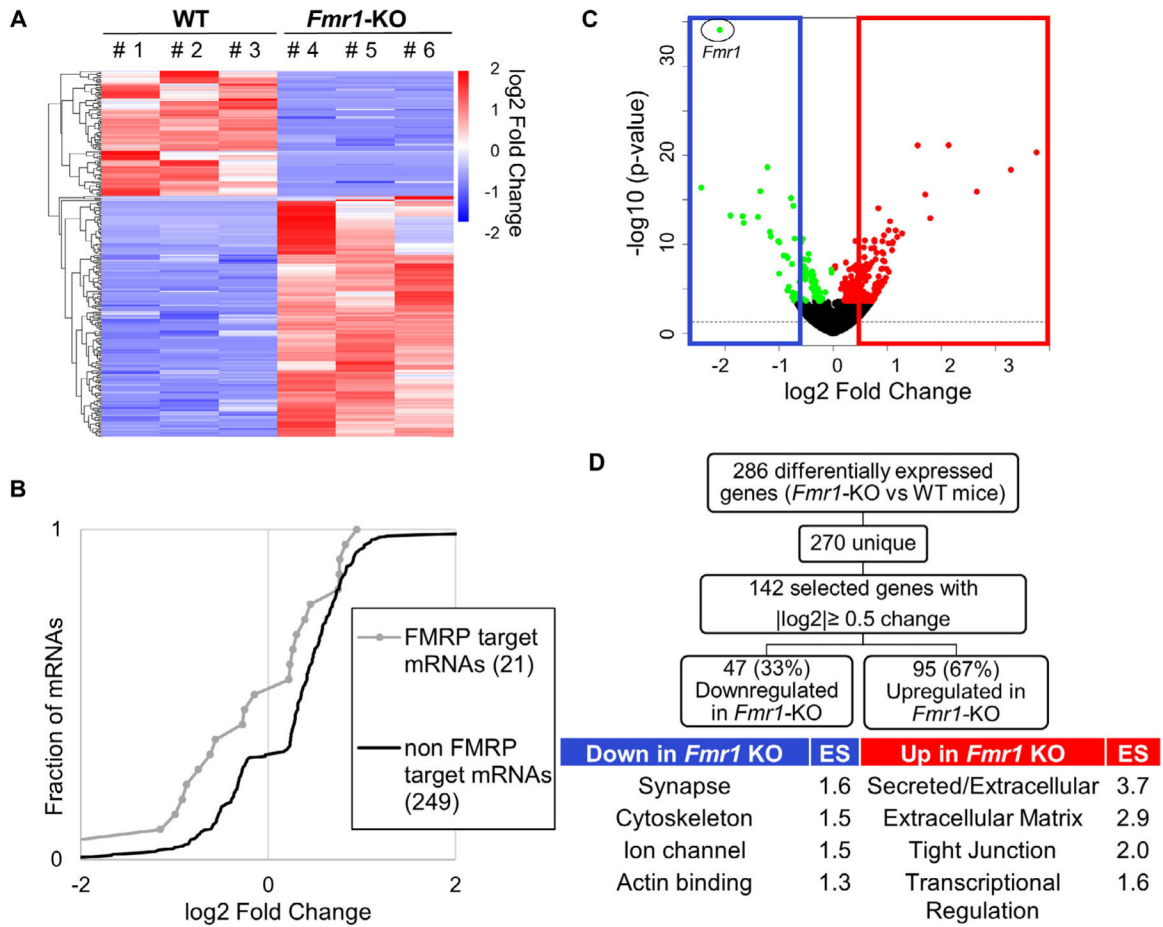
## BIBLIOGRAPHY

1. Darnell JC, Klann E. The translation of translational control by FMRP: therapeutic targets for FXS. *Nat Neurosci* 2013;16:1530–1536. [PubMed: 23584741]
2. Irwin SA, Galvez R, Greenough WT. Dendritic spine structural anomalies in fragile-X mental retardation syndrome. *Cereb Cortex* 2000;10:1038–1044. [PubMed: 11007554]
3. Fu YH, Kuhl DP, Pizzuti A, et al. Variation of the CGG repeat at the fragile X site results in genetic instability: resolution of the Sherman paradox. *Cell* 1991;67:1047–1058. [PubMed: 1760838]
4. Hagerman PJ. The fragile X prevalence paradox. *J Med Genet* 2008;45: 498–499. [PubMed: 18413371]
5. Rotschafer SE, Razak KA. Auditory processing in fragile x syndrome. *Front Cell Neurosci* 2014;8:19. [PubMed: 24550778]
6. Fmr1 knockout mice: a model to study fragile X mental retardation. The Dutch-Belgian fragile X consortium. *Cell* 1994;78:23–33. [PubMed: 8033209]
7. Chen L, Toth M. Fragile X mice develop sensory hyperreactivity to auditory stimuli. *Neuroscience* 2001;103:1043–1050. [PubMed: 11301211]
8. Yan QJ, Rammal M, Tranfaglia M, Bauchwitz RP. Suppression of two major fragile X syndrome mouse model phenotypes by the mGluR5 antagonist MPEP. *Neuropharmacology* 2005;49:1053–1066. [PubMed: 16054174]
9. Yun SW, Platholi J, Flaherty MS, Fu W, Kottmann AH, Toth M. Fmrp is required for the establishment of the startle response during the critical period of auditory development. *Brain Res* 2006;1110:159–165. [PubMed: 16887106]
10. Gonzalez D, Tomasek M, Hays S, et al. Audiogenic seizures in the Fmr1 Knock-out mouse are induced by Fmr1 deletion in subcortical, VGlut2-expressing excitatory neurons and require deletion in the inferior colliculus. *J Neurosci* 2019;39:9852–9863. [PubMed: 31666356]
11. Wang Y, Sakano H, Beebe K, et al. Intense and specialized dendritic localization of the fragile X mental retardation protein in binaural brainstem neurons: a comparative study in the alligator, chicken, gerbil, and human. *J Comp Neurol* 2014;522:2107–2128. [PubMed: 24318628]
12. Brew HM, Hallows JL, Tempel BL. Hyperexcitability and reduced low threshold potassium currents in auditory neurons of mice lacking the channel subunit Kv1.1. *J Physiol* 2003;548:1–20. [PubMed: 12611922]
13. Brew HM, Gittelman JX, Silverstein RS, et al. Seizures and reduced life span in mice lacking the potassium channel subunit Kv1.2, but hypoexcitability and enlarged Kv1 currents in auditory neurons. *J Neurophysiol* 2007;98:1501–1525. [PubMed: 17634333]
14. Ison JR, Allen PD, Tempel BL, Brew HM. Sound localization in Preweanling mice was more severely affected by deleting the Kcna1 gene compared to deleting Kcna2, and a curious inverted-U course of development that appeared to exceed adult performance was observed in all groups. *J Assoc Res Otolaryngol* 2019;20:565–577. [PubMed: 31410614]
15. Huang da W, Sherman BT, Lempicki RA. Systematic and integrative analysis of large gene lists using DAVID bioinformatics resources. *Nat Protoc* 2009;4:44–57. [PubMed: 19131956]
16. Litovchick L. Immunoblotting. *Cold Spring Harb Protoc* 2020;2020: 098392. [PubMed: 32482904]
17. Brown V, Jin P, Ceman S, et al. Microarray identification of FMRP-associated brain mRNAs and altered mRNA translational profiles in fragile X syndrome. *Cell* 2001;107:477–487. [PubMed: 11719188]
18. Darnell JC, Van Driesche SJ, Zhang C, et al. FMRP stalls ribosomal translocation on mRNAs linked to synaptic function and autism. *Cell* 2011; 146:247–261. [PubMed: 21784246]
19. Donnard E, Shu H, Garber M. Single cell transcriptomics reveals dysregulated cellular and molecular networks in a fragile X syndrome model. *PLoS Genet* 2022;18:e1010221. [PubMed: 35675353]
20. Auerbach BD, Rodrigues PV, Salvi RJ. Central gain control in tinnitus and hyperacusis. *Front Neurol* 2014;5:206. [PubMed: 25386157]
21. Allen Brain Atlas Available at: <https://portal.brain-map.org/>.

22. Heilstedt HA, Burgess DL, Anderson AE, et al. Loss of the potassium channel beta-subunit gene, KCNAB2, is associated with epilepsy in patients with 1p36 deletion syndrome. *Epilepsia* 2001;42:1103–1111. [PubMed: 11580756]
23. Perkowski JJ, Murphy GG. Deletion of the mouse homolog of KCNAB2, a gene linked to monosomy 1p36, results in associative memory impairments and amygdala hyperexcitability. *J Neurosci* 2011;31:46–54. [PubMed: 21209188]
24. Nakahira K, Shi G, Rhodes KJ, Trimmer JS. Selective interaction of voltage-gated K<sup>+</sup> channel beta-subunits with alpha-subunits. *J Biol Chem* 1996;271:7084–7089. [PubMed: 8636142]
25. Friedland DR, Eernisse R, Popper P. Potassium channel gene expression in the rat cochlear nucleus. *Hear Res* 2007;228:31–43. [PubMed: 17346910]
26. Rotschafer S, Razak K. Altered auditory processing in a mouse model of fragile X syndrome. *Brain Res* 2013;1506:12–24. [PubMed: 23458504]
27. Frankland PW, Wang Y, Rosner B, et al. Sensorimotor gating abnormalities in young males with fragile X syndrome and Fmr1-knockout mice. *Mol Psychiatry* 2004;9:417–425. [PubMed: 14981523]
28. Fields RD, Woo DH, Basser PJ. Glial regulation of the neuronal connectome through local and long-distant communication. *Neuron* 2015;86:374–386. [PubMed: 25905811]
29. MacKinnon R Determination of the subunit stoichiometry of a voltage-activated potassium channel. *Nature* 1991;350:232–235. [PubMed: 1706481]
30. Rusznak Z, Bakondi G, Pocsai K, et al. Voltage-gated potassium channel (Kv) subunits expressed in the rat cochlear nucleus. *J Histochem Cytochem* 2008;56:443–465. [PubMed: 18256021]
31. Heinemann SH, Rettig J, Graack HR, Pongs O. Functional characterization of Kv channel beta-subunits from rat brain. *J Physiol* 1996;493(Pt 3): 625–633. [PubMed: 8799886]
32. Yoshimura H, Takumi Y, Nishio SY, Suzuki N, Iwasa Y, Usami S. Deafness gene expression patterns in the mouse cochlea found by microarray analysis. *PLoS One* 2014;9:e92547. [PubMed: 24676347]
33. Rhodes KJ, Monaghan MM, Barrezueta NX, et al. Voltage-gated K<sup>+</sup> channel beta subunits: expression and distribution of Kv beta 1 and Kv beta 2 in adult rat brain. *J Neurosci* 1996;16:4846–4860. [PubMed: 8756417]
34. Jastreboff PJ, Sasaki CT. Salicylate-induced changes in spontaneous activity of single units in the inferior colliculus of the Guinea pig. *J Acoust Soc Am* 1986;80:1384–1391. [PubMed: 3782617]
35. Sun W, Zhang L, Lu J, Yang G, Landrie E, Salvi R. Noise exposure-induced enhancement of auditory cortex response and changes in gene expression. *Neuroscience* 2008;156:374–380. [PubMed: 18713646]
36. Kaltenbach JA, Afman CE. Hyperactivity in the dorsal cochlear nucleus after intense sound exposure and its resemblance to tone-evoked activity: a physiological model for tinnitus. *Hear Res* 2000;140:165–172. [PubMed: 10675644]
37. Boettcher FA, Salvi RJ. Functional changes in the ventral cochlear nucleus following acute acoustic overstimulation. *J Acoust Soc Am* 1993;94:2123–2134. [PubMed: 8227752]
38. Sun S, Siebald C, Muller U. Subtype maturation of spiral ganglion neurons. *Curr Opin Otolaryngol Head Neck Surg* 2021;29:391–399. [PubMed: 34412064]
39. gEAR (gene Expression Analysis Resource) Available at: <https://umgear.org/>.

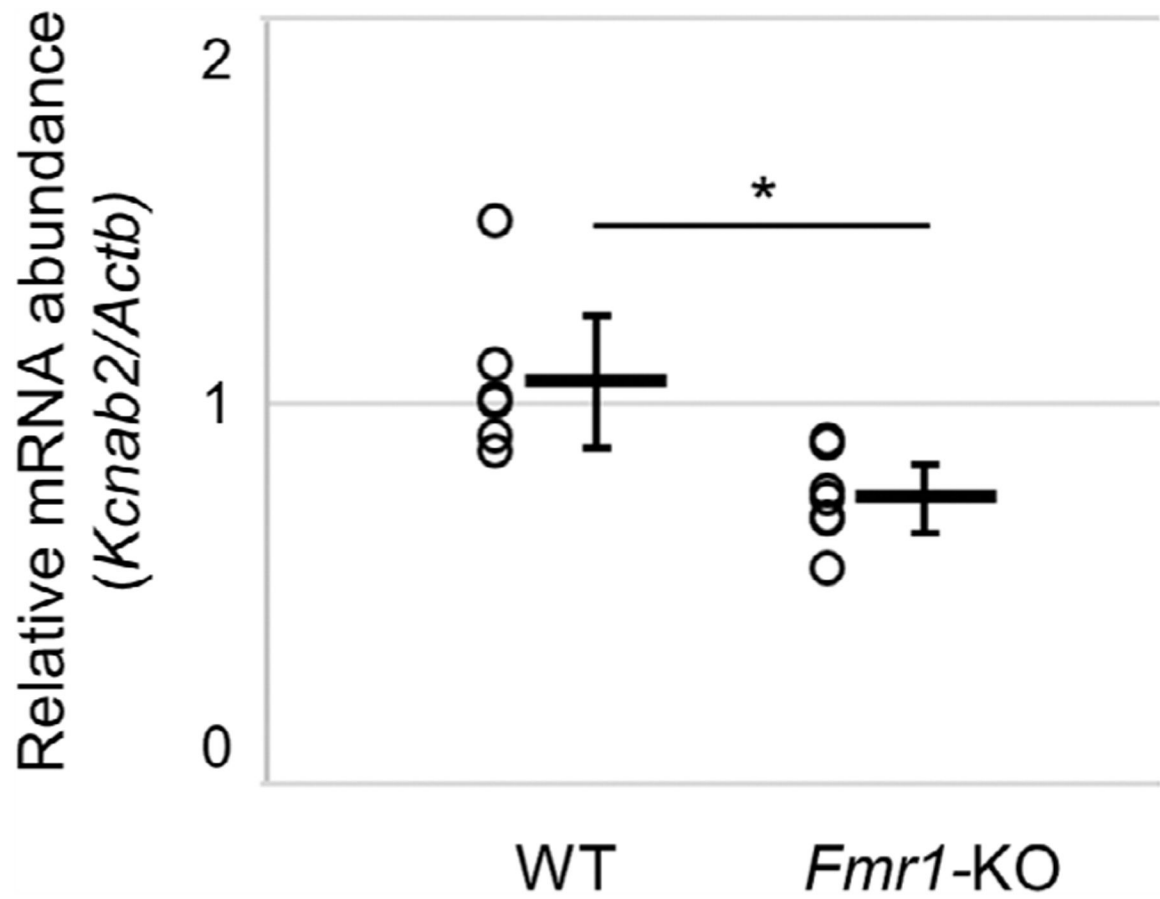


**FIGURE 1.** Fragile X Protein (FMRP) immunostaining of cochlear nucleus. (A) Strong FMRP expression in WT cochlear nucleus that is (B) absent in the *Fmr1*-KO. (C) Delineation (dotted line) of a surgically excised cochlear nucleus (CN) from a coronal slice of brainstem with (D) intact side shown as a reference. Scale bars = 200  $\mu$ m.



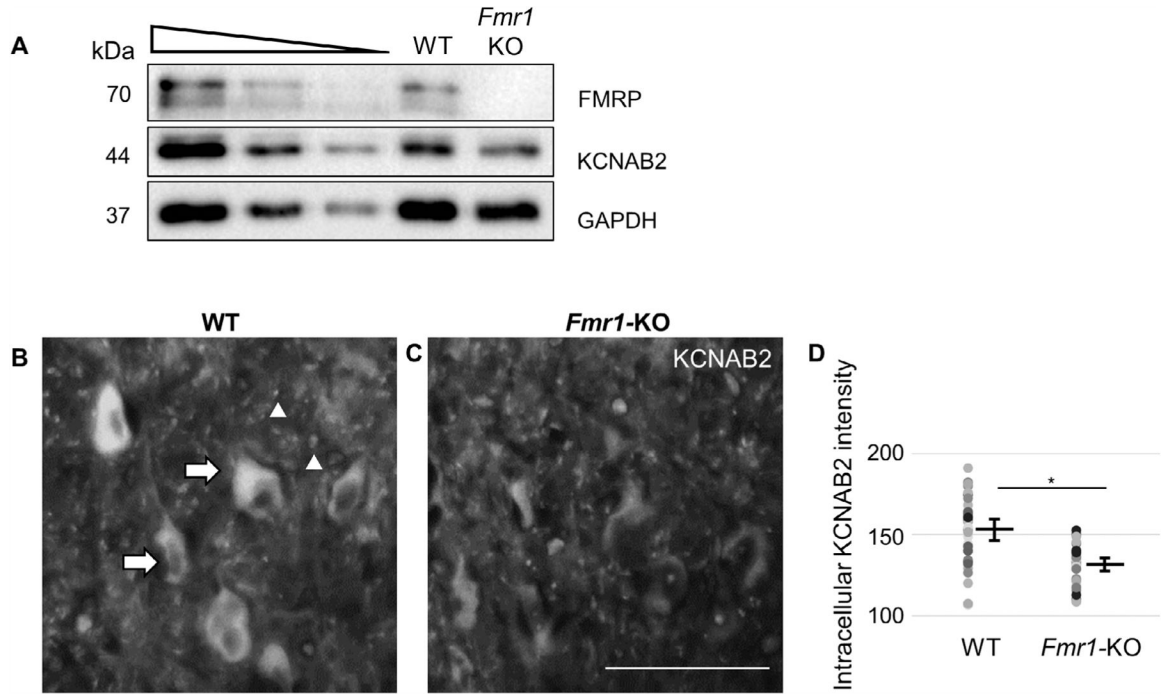
**FIGURE 2.**

Altered gene expression in *Fmr1*-KO compared to WT cochlear nucleus. (A) Heat map of cochlear nuclei transcripts that are either upregulated (red) or downregulated (blue) in *Fmr1*-KO (columns #4–6) compared to WT mice (columns #1–3). Three biological replicates, each generated from pooling the cochlear nuclei of two mice, were used for each genotype. (B) Distribution plot of the fraction of differentially expressed genes and their log2 fold differences between *Fmr1*-KO and WT for known targets of Fragile X Protein (FMRP (gray)) versus others (black). FMRP targets are downregulated overall compared to non-targets shown by a leftward shift in the distribution curve. (C) Volcano plot showing the logarithmic distribution of genes based on fold-difference versus p-value. Circle denotes *Fmr1*, whose partial transcript is detected in the *Fmr1*-KO mice. The boxed area represents genes with at least |log2| ≥ 0.5-fold difference that were selected for gene ontology analyses. (D) Gene ontology performed using DAVID program for enrichment analysis. (ES = enrichment score).

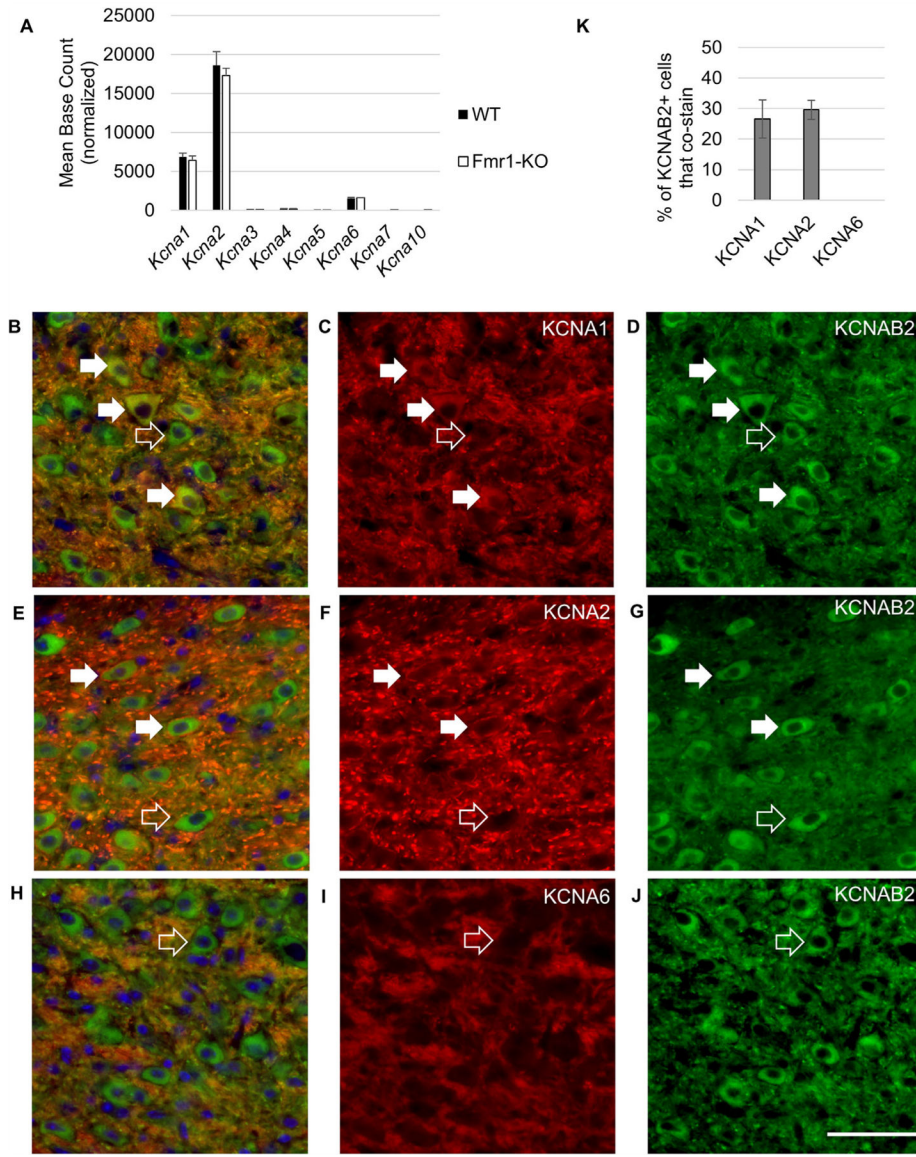


**FIGURE 3.**

Quantitation of *Kcnab2* mRNA by RT-qPCR. Comparison of WT and *Fmr1*-KO cochlear nuclei shows a statistically significant difference in *Kcnab2* mRNA abundance when normalized to the control *Actb*: 1.06 (95% CI [0.88,1.23],  $n = 6$ ) versus 0.75 (95% CI [0.66,0.84],  $n = 7$ ), respectively. Individual data represented by open circles, bar = averages, error bars = 95% confidence intervals, (\*)  $p < 0.01$ , Student's t-test.

**FIGURE 4.**

KCNAB2 expression in the cochlear nucleus. (A) Western blotting of cochlear nucleus lysate for KCNAB2 and Fragile X Protein (FMRP). GAPDH shown as loading control. (B) Immunostaining for KCNAB2 in the WT cochlear nucleus is within a subset of cells (arrows). Punctate staining also seen in neurites (arrowhead). (C) KCNAB2 in the *Fmr1*-KO is reduced compared to that in WT. (D) Intensity of KCNAB2 staining within positive cells is reduced by 21 points in the *Fmr1*-KO mice (131.51, 95% CI [127.33,135.69],  $n = 35$ ) compared to WT (152.95, 95% CI [146.24,159.66],  $n = 41$ ). Individual cell data shown in circles, bar = averages, error bars = 95% confidence intervals, (\*)  $p < 0.01$ , Student's t-test, scale bar, 100  $\mu\text{m}$ .

**FIGURE 5.**

KCNAB2 co-expression with KCNA1 and 2, but not 6. (A) mRNA levels of all Shaker  $\alpha$  subunits from mouse cochlear nucleus using the RNA-seq normalized base count for WT (black) and *Fmr1*-KO (white) ( $n = 3$  each). *Kcna1* and *Kcna2* are the most abundant while *Kcna6* barely detectable. There was no statistically significant difference between *Fmr1*-KO and WT by Student's *t*-test. (B–J) Ventral cochlear nuclei from adult WT mice were co-immunostained for KCNAB2 and KCNA1 (B–D), KCNA2 (E–G) or KCNA6 (H–J) ( $n > 120$  cells for each, solid arrows indicate co-expression, empty arrows indicate no co-expression). Individual fluorescence channels for the  $\alpha$  subunit are shown in the middle column and for the  $\beta$  subunit are shown in the right column. KCNAB2 co-stained frequently with KCNA1 (solid arrows). KCNAB2 also co-stained with KCNA2. KCNA2 appeared to be localized along the plasma membrane. KCNAB2 did not co-stain with KCNA6 (empty arrows). (J) Quantitation of KCNAB2+ cells reveals that approximately one-third are KCNA1+ and

one-third are KCNA2+. KCNA6 co-staining was not detectable. Scale bar = 50  $\mu$ m. Error bars = standard deviation.

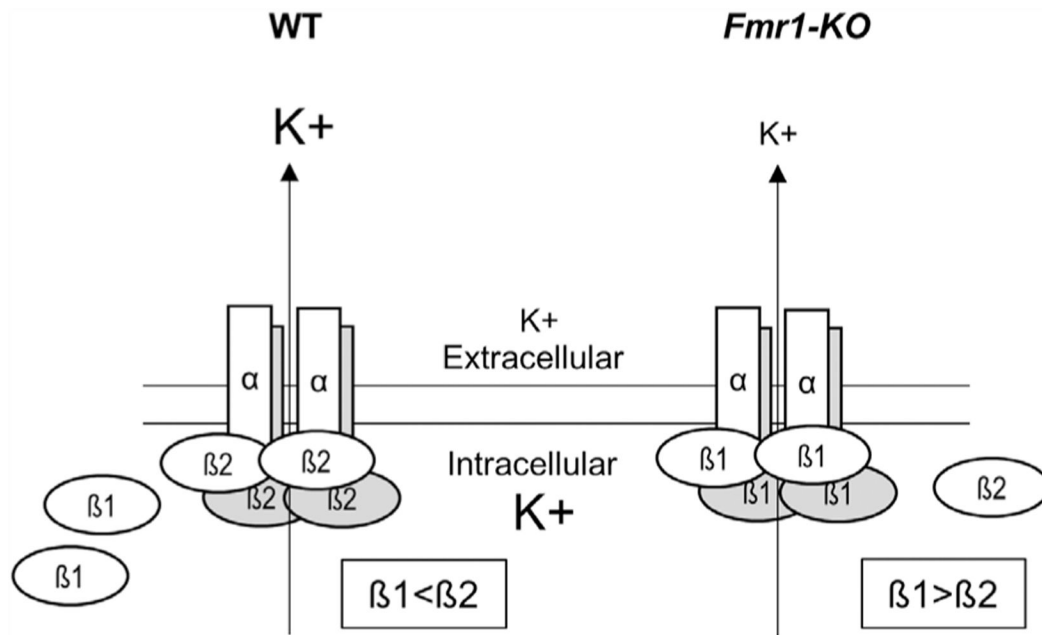
Author Manuscript

Author Manuscript

Author Manuscript

Author Manuscript





- More  $\beta 2$ , competes with  $\beta 1 \rightarrow$
1. Lowers the activation threshold such that the channel opens at a more hyperpolarized state
  2.  $\beta 2$  lacks the inactivation domain  $\rightarrow$  prolonged potassium efflux
  3. Results in faster repolarization

- Less  $\beta 2$ , unopposed  $\beta 1 \rightarrow$
1. Activation threshold is above the action potential
  2.  $\beta 1$  has a ball and chain domain to allow for inactivation
  3. Results in prolonged action potential and hyper-excitability

**FIGURE 6.**

Schematic of what may occur with an abnormally reduced abundance of the KCNAB2 subunit ( $\beta 2$ ). KCNAB2 interacts with each of the pore-forming  $\alpha$  subunits of the Shaker family voltage-gated potassium channels that form a heterotetramer ( $\alpha$ ). In the WT, KCNAB2 ( $\beta 2$ ) competes with KCNAB1 ( $\beta 1$ ) and lowers the activation threshold, and does not inactivate the channel, resulting in faster repolarization of the neuron. In the *Fmr1-KO*, a reduction in KCNAB2 allows unopposed KCNAB1 to increase the activation threshold and then inactivate the channel, resulting in prolonged action potential and hyper-excitability of the neuron.

TABLE I.

Antibodies Used in this Study.

Detects	Antigen	Host, Dilution	Catalogue	RRID
FMRP	Human FMRP	Rabbit, polyclonal	Abcam, ab17722	AB_2278530
KCNAB2	aa550-C-term Rat Kvβ2 aa20–34	1:1000 (W), 1:500 (IHC) Rabbit polyclonal	Alomone Lab, APC-117	AB_2039961
GAPDH	Human GAPDH C-term	1:2000 (W), 1:450 (IHC) Rabbit monoclonal 14C10 1:200 (W)	Cell Signaling, 2118	AB_10693448

aa, amino acid; IHC, immunohistochemistry; W, western blotting.

List of Synaptic Pathway-related Genes that were Abnormally Decreased in Expression in the Cochlear Nucleus of *Fmr1*-KO Mice.

**TABLE II.**

Genes	Aliases	Description	Log <sub>2</sub>	Base mean	Allen Brain Atlas	FMRP bound
Piezo1	DHS, FAM38A, Mib, LMPH3	Mechanosensitive ion channel	-1.657	55	Yes	No
Kcnp4	CALP, KCHIP4	Voltage-gated potassium channel interacting protein 4	-1.348	172	Yes	No
Gria3	GlutR3, AMPAR3	AMPA receptor subunit	-1.001	311	Yes	No
Kcnab2	Kvβ2, HK-βbeta2	Voltage-gated, Shaker-related subfamily, beta member 2	-0.781	1998	Yes	No
Clcn7	Clc7, Opta2, Optb4	Voltage-gated chloride channel 7	-0.615	681	Yes	No
Pacsin1		PKC substrate regulates KCC2	-0.559	795	Yes	No

All genes were confirmed for expression in the adult mouse cochlear nucleus using the Allen Brain Atlas<sup>21</sup> which is an online database of in-situ hybridization of mouse and human brain. Fragile X Protein (FMRP) bound targets are defined by previous studies using FMRP cross-linking immunoprecipitation.<sup>17,18</sup>